

Neutrino scattering and B anomalies from hidden sector portals

Alakabha Datta,^{a,b} Bhaskar Dutta,^c Shu Liao,^c Danny Marfatia^d and Louis E. Strigari^c

^a*Department of Physics and Astronomy, 108 Lewis Hall, University of Mississippi, Oxford, MS 38677-1848, USA*

^b*Department of Physics and Astronomy, University of California, 4129 Frederick Reines Hall, Irvine, CA 92697-4575, USA*

^c*Mitchell Institute for Fundamental Physics and Astronomy, Department of Physics and Astronomy, Texas A&M University, 4242 TAMU, College Station, TX 77845, USA*

^d*Department of Physics and Astronomy, University of Hawaii-Manoa, 2505 Correa Road, Honolulu, HI 96822, USA*

ABSTRACT: We examine current constraints on and the future sensitivity to the strength of couplings between quarks and neutrinos in the presence of a form factor generated from loop effects of hidden sector particles that interact with quarks via new interactions. We consider models associated with either vector or scalar interactions of quarks and leptons generated by hidden sector dynamics. We study constraints on these models using data from coherent elastic neutrino-nucleus scattering and solar neutrino experiments and demonstrate how these new interactions may be discovered by utilizing the recoil spectra. We show that our framework can be naturally extended to explain the lepton universality violating neutral current B decay anomalies, and that in a model framework the constraints from neutrino scattering can have implications for these anomalies.

Contents

1	Introduction	1
2	Form factors	2
2.1	Z' Model	2
2.2	S Model	4
3	Scattering cross sections	5
4	Experimental bounds	6
4.1	Accelerators and reactors	6
4.2	Solar neutrinos	8
5	B anomalies	10
6	Conclusions	15

1 Introduction

In spite of the success of the standard model (SM) in describing the particle interactions observed in nature, neutrino interactions with matter are not thoroughly understood. Many experiments are now making precise measurements of neutrino-nucleus scattering cross sections and neutrino-electron elastic scattering cross sections. The measurements are now precise enough that they are able to probe beyond the SM physics. Recently, the COHERENT experiment at the Spallation Neutron Source (SNS) has measured coherent elastic neutrino-nucleus scattering (CE ν NS) for the first time, finding that the cross section for scattering on CsI is consistent with the SM at approximately 1σ [1]. In addition, measurements by Borexino of the solar neutrino flux, in particular the ${}^7\text{Be}$ component, now provide the best measurement of the neutrino-electron elastic scattering cross section at electron recoil energies $\lesssim \text{MeV}$ [2].

Because of this plethora of current and future experimental data, it is imperative to consider new theoretical ideas for neutrino interactions in these low energy experiments. Consider axial-vector interactions between quarks and neutrinos mediated by a new Z' boson. We write the interaction of the quarks with the Z' as,

$$\mathcal{L}_{q'q'} = \bar{q}'\gamma^\mu [P_L F_L(q^2) + P_R F_R(q^2)] q' Z'_\mu, \quad (1.1)$$

where $\gamma^\mu = \left[\gamma_\mu - \frac{\gamma \cdot q q^\mu}{q^2}\right]$ and q' are SM quark fields. The interaction of the Z' with the leptons has an analogous expression. In the interaction above, the contribution from the q^μ part may be suppressed by small masses or vanish from current conservation. Form factors

proportional to $\sigma^{\mu\nu}q_\nu$ are possible, but will be suppressed by some hadronic scale; we do not investigate these in this paper.

The form factor $F(q^2)$ can be unity when q' couples directly to Z' . However, in many models (especially the models with low scale hidden sectors), q' may couple to Z' via a loop containing DM/hidden sector particles. In such a scenario we expect $F(q^2) \sim q^2/\Lambda^2$ where Λ is the scale in the DM sector associated with the mass of the mediator particle that generates the quark-DM interactions, $\bar{q}q\bar{\chi}\chi$. As long as Λ is greater than q_{max} for these scattering experiments, $F(q^2) \sim q^2/\Lambda^2$ appears in the scattering amplitude. In this paper, we investigate these new form factors at CE ν NS (COHERENT and reactor based) and Borexino experiments for vector and scalar mediators. We extend our framework to study the neutral current B decay anomalies in the R_K and R_{K^*} measurements. We show how in a model framework measurements from neutrino scattering may have implications for the B anomalies.

The paper is organized as follows. In Section II, we discuss models for form factors and their dependence on the new physics scale. In Sections III and IV we discuss the effects of these new form factors at CE ν NS and Borexino experiments, respectively. In Section V we discuss the B anomalies and the implications of neutrino scattering experiments on their explanations. We conclude in Section VI.

2 Form factors

2.1 Z' Model

Consider the following Lagrangian at low energy [3]:

$$\begin{aligned}\mathcal{L} &= \frac{g}{\Lambda^2} \bar{q}' \gamma^\mu P_{L,R} q' \bar{\chi} \gamma_\mu (1 \pm \gamma_5) \chi + i \bar{\chi} \gamma^\nu [\partial_\nu - i g_\chi Z'^\nu] \chi - m_\chi \bar{\chi} \chi + \frac{1}{2} m_{Z'}^2 Z'_\mu Z'^\mu \\ &= H_{eff} + J_{\mu,\chi} Z'^\mu + i \bar{\chi} \gamma^\nu \partial_\nu \chi - m_\chi \bar{\chi} \chi + \frac{1}{2} m_{Z'}^2 Z'_\mu Z'^\mu,\end{aligned}\quad (2.1)$$

where χ is a hidden sector fermion field with mass m_χ . The first term in the Lagrangian represents an effective coupling between the q and χ fields that might arise through the exchange of a heavy mediator of mass $\sim \Lambda$, with $\Lambda \gg E$, where E is the energy scale of the process (see for example [4–6]). The hidden sector fields χ couple directly to Z' through the vector portal and so in our framework there are two mediators; see e.g., [7]. We further assume that the neutrinos are charged under the $Z' U(1)$ and so there is a direct coupling of the neutrinos to Z' . Although there is no direct coupling between the quarks and Z' field, a χ -loop-induced $\bar{q}qZ'$ effective vertex (as in Eq. 1.1) will be generated with a q^2 dependent coupling, which can be represented by a higher dimensional operator,

$$\mathcal{L}_{HD} = \frac{g_{L,R}}{\Lambda^2} \bar{q}' \gamma^\mu P_{L,R} q' \partial^\nu Z'_{\mu\nu}, \quad (2.2)$$

where $Z'_{\mu\nu}$ is the Z' field tensor; see Fig. 1. This higher dimensional operator may be considered to be the bare term of the Lagrangian.

The form factors in Eq. (1.1) are then given by

$$\bar{q}' \hat{\gamma}^\mu [P_L F_L(q^2) + P_R F_R(q^2)] q' = \frac{1}{\Lambda^2} \langle q' | \int d^4x e^{iq \cdot x} T [J_{\mu,\chi}(x) H_{eff}(0)] | q' \rangle. \quad (2.3)$$

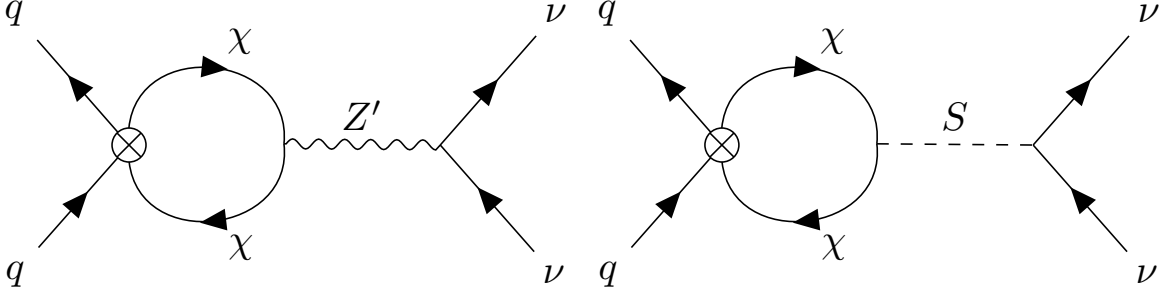


Figure 1. Feynman diagram for Z' model (left) and S model (right).

The most general structure for the form factors from the current conservation of $J_{\mu,\chi}$ is

$$\begin{aligned} F_L(q^2) &= \frac{q^2}{\Lambda^2} A_L(q^2), \\ F_R(q^2) &= \frac{q^2}{\Lambda^2} A_R(q^2). \end{aligned} \quad (2.4)$$

Since the matrix element in Eq. (2.3) is finite as $q^2 \rightarrow 0$, $A_{L,R}(q^2)$ is finite as $q^2 \rightarrow 0$. Now from Eqs. (2.2) and (2.3), we can estimate the form factor in the 1-loop approximation [8]. We get

$$F_{L,R}(q^2) = \frac{q^2}{\Lambda^2} \left[g_{L,R} + gg_\chi \frac{1}{(2\pi)^4} \int_0^1 dx \, 8x(1-x) \int d^4l \frac{1}{(l^2 - \Delta + i\epsilon)^2} \right], \quad (2.5)$$

where $\Delta = m_\chi^2 - q^2 x(1-x)$. Introducing a cut-off Λ_c to regulate the divergent integral we can write

$$\begin{aligned} F_{L,R}(q^2) &= \frac{q^2}{\Lambda^2} \left[g_{L,R} + \frac{gg_\chi}{2\pi^2} \int_0^1 dx \, x(1-x) \ln \frac{x\Lambda_c^2}{\Delta} \right], \\ &= \frac{q^2}{\Lambda^2} g_{L,R}(q^2). \end{aligned} \quad (2.6)$$

where g and g_χ are the bare coupling constants. We rewrite $g_{L,R}(q^2)$ as

$$g_{L,R}(q^2) = g_{L,R}(q_{max}^2) + \frac{gg_\chi}{2\pi^2} \int_0^1 dx \, x(1-x) \ln \frac{\Delta_{max}}{\Delta}, \quad (2.7)$$

where $\Delta_{max} = m_\chi^2 - q_{max}^2 x(1-x)$ and q_{max}^2 is the maximum momentum transfer squared.

Note that this is a rough estimate as we have calculated only the leading term in Eq. (2.3). However, the general structure of Eq. (2.4) still holds as it follows from vector current conservation. As a rough estimate, assuming all terms in Eq. (2.7) to be of the same size, we can write,

$$g_{L,R}(q^2) \sim \frac{gg_\chi}{2\pi^2} \int_0^1 dx \, x(1-x) \ln \frac{\Delta_{max}}{\Delta}. \quad (2.8)$$

For our purposes, the most important part of Eq. (2.5) is the q^2/Λ^2 factor which is not present if either the tree level (first term) or the loop contribution (second term) is

absent; the latter is Eq. (2.8). We show both tree and loop contributions since each term may not be sizable in a given model. The relative strength between the tree and the loop contributions does not affect our analysis.

Although the Lagrangian in Eq. (2.1) contains both g_L and g_R terms, only $g_L + g_R \equiv g_v$ contributes to ν -nucleus coherent scattering; $g_L - g_R \equiv g_a$ does not impact the scattering process. This is because the vector charge of the nucleus is proportional to the number of nucleons, $Q_v = Zg_v^p + Ng_v^n$ while the axial vector couplings are proportional to the spin, $Q_a = g_a^p \langle S_p \rangle + g_a^n \langle S_n \rangle$ which is much smaller than Q_v .

2.2 S Model

As for the Z' case the form factors for a scalar mediator S can be written as

$$\bar{q}' [P_L S_L(q^2) + P_R S_R(q^2)] q' = \frac{1}{\Lambda^2} \langle q' | \int d^4x e^{iq \cdot x} T [J_\chi(x) H_{eff}(0)] | q' \rangle, \quad (2.9)$$

where

$$\begin{aligned} H_{eff} &= \frac{g}{\Lambda^2} \bar{q} P_{L,R} q \bar{\chi} (1 \pm \gamma_5) \chi, \\ J_\chi &= \bar{\chi} [g_\chi P_L + g'_\chi P_R] \chi. \end{aligned} \quad (2.10)$$

In this case we cannot use current conservation. By calculating the leading loop contribution we find,

$$S_{L,R}(q^2) = gg_\chi \frac{1}{(2\pi)^4} \int_0^1 dx \, 12x(1-x) \frac{\Delta}{\Lambda^2} \int d^4l \frac{1}{(l^2 - \Delta + i\epsilon)^2}. \quad (2.11)$$

Again introducing a cut-off Λ_c we can write,

$$S_{L,R}(q^2) \sim \frac{3gg_\chi}{4\pi^2} \int_0^1 dx \, x(1-x) \frac{[m_\chi^2 - q^2x(1-x)]}{\Lambda^2} \ln \frac{x\Lambda_c^2}{\Delta}. \quad (2.12)$$

For $m_\chi^2 \ll q^2$, $S_{L,R}(q^2) \sim q^2$. Unlike the Z' case the form factor is sensitive to the χ mass and so the hidden sector dynamics can be probed in low energy scattering.

A scalar coupling has a larger effect on the coherent scattering rate $\sim O(E_R)$, compared to the rate from a pseudoscalar coupling, $\frac{1}{8\pi p^2} \frac{g_v^2 g_q^2}{(2m_N E_R + m_s^2)^2} E_R^2 m_N \sim O(E_R^2)$.

The scalar interactions of quarks with dark matter $\sim \frac{g}{\Lambda^2} \bar{q} P_{L,R} q \bar{\chi} P_{L,R} \chi$ could arise from a higher dimensional operator $\frac{g}{\Lambda^3} H \bar{q} P_{L,R} q \bar{\chi} P_{L,R} \chi$. With the assumption of minimal flavor violation (MFV) this interaction has the form $\sim \frac{m_q}{\Lambda^3} \bar{q} P_{L,R} q \bar{\chi} P_{L,R} \chi$ [4].

It is worth considering how the phenomenology changes if one uses MFV to constrain the scalar interactions. Without MFV the matrix element that appears in the amplitude is $M \sim \langle N | \bar{q} q | N \rangle$ while with MFV we need $M' \sim \frac{1}{\Lambda} \langle N | m_q \bar{q} q | N \rangle$. If the heavy c, b, t quarks are involved they can be integrated out and their contributions replaced by a gluonic term [9, 10]. If contributions arise only from the light quarks then $\frac{M'}{M} \sim \frac{m_q}{\Lambda}$, and for $\Lambda \gg m_q$ the matrix element for the MFV case is suppressed. Hence, the bounds on Λ from coherent scattering will be weaker.

When we discuss the B anomalies below, we will require that dark matter couple to quarks of all generations or at least to all generations of down quarks. Consequently, the

heavy quarks could contribute to coherent scattering via the gluonic terms. However, for the B anomalies we need a flavor changing coupling g_{bs} which involves a mixing angle. In other words, the B anomalies do not completely fix the coupling g_q , of the heavy quarks to dark matter. The heavy quark contribution to the matrix element M goes as $\sim g_q \frac{m_N}{m_q}$ while for M' it goes as $\sim g_q \frac{m_N}{\Lambda}$, where m_N is the nucleon mass.

Note that the scalar coupling to the neutrinos may originate from the lepton number violating interaction, $\phi \bar{\nu}_L^c \nu_L$, or from the lepton number conserving interaction, $\phi \bar{\nu}_R \nu_L$, where ϕ is a SM scalar singlet. If ϕ is a pseudoscalar, then the associated coupling is not constrained by coherent scattering but is constrained by $\pi^0 \rightarrow \bar{\nu} \nu$ [11] to be smaller than 10^{-5} .

Finally, depending on whether or not right-handed neutrinos are present, we can write neutrino-quark interaction terms as $g'/m'^2 \bar{\nu}_R \nu_L \bar{q} q$ or $g'/m'^2 \bar{\nu}_L^c \nu_L \bar{q} q$. If the second term is present, then a Majorana mass term arises from the quark condensate, i.e., $m_\nu = g'/(m'/\text{GeV})^2 \bar{q} q = g'/(m'/\text{GeV})^2 10^7 \text{ eV}$ with $\bar{q} q = 8\pi/\sqrt{3} f_\pi^3$ as calculated in the Nambu-Jona-Lasinio model [12]. Since the heaviest neutrino mass is $\sim 0.1 \text{ eV}$, we find $g'/(m'/\text{GeV})^2 \leq 10^{-8}$. However, g' is constrained by COHERENT to be smaller than 10^{-10} (10^{-8}) for $m' = 10 \text{ MeV}$ (1 GeV) [13].

3 Scattering cross sections

For the vector model we can write the effective interaction as

$$\mathcal{L}_{\text{BSM}} = -2\sqrt{2}G_F \bar{\nu}_L \gamma^\mu \nu_L \bar{f} \gamma_\mu f \frac{g'F(q^2, \Lambda^2)}{q^2 + m'^2} \frac{1}{2\sqrt{2}G_F}, \quad (3.1)$$

where $F(q^2, \Lambda^2) = \frac{q^2}{\Lambda^2}$. Since the vector interaction has the same structure as in the SM, its contribution can interfere with the SM contribution.

The neutrino-electron differential cross section can be written as

$$\frac{d\sigma}{dE_R} = \frac{2}{\pi} G_F^2 m_e \left[(\epsilon^L)^2 + (\epsilon^R)^2 \left(1 - \frac{E_R}{E_\nu}\right)^2 - \epsilon^L \epsilon^R \frac{m_e E_R}{E_\nu^2} \right], \quad (3.2)$$

where $\epsilon^L = \frac{1}{2} + \sin^2 \theta_w + \frac{g'F(q^2, \Lambda^2)}{q^2 + m'^2} \frac{1}{2\sqrt{2}G_F}$ and $\epsilon^R = \sin^2 \theta_w + \frac{g'F(q^2, \Lambda^2)}{q^2 + m'^2} \frac{1}{2\sqrt{2}G_F}$ for the electron neutrino, and $\epsilon^L = -\frac{1}{2} + \sin^2 \theta_w + \frac{g'F(q^2, \Lambda^2)}{q^2 + m'^2} \frac{1}{2\sqrt{2}G_F}$ and $\epsilon^R = \sin^2 \theta_w + \frac{g'F(q^2, \Lambda^2)}{q^2 + m'^2} \frac{1}{2\sqrt{2}G_F}$ for the muon or tau neutrino.

The neutrino-nucleus differential cross section is

$$\frac{d\sigma}{dE_R} = \frac{2}{\pi} G_F^2 m_N Q_V^2 \left[1 - \frac{m_N E_R}{E_\nu^2} + \left(1 - \frac{E_R}{E_\nu}\right)^2 \right] F_{\text{nucl}}(q^2), \quad (3.3)$$

where $F_{\text{nucl}}(q^2)$ is the nuclear form factor, the “weak charge” Q_V is given by

$$Q_V = \frac{1}{2} \left[Z \left(\frac{1}{2} - 2\sin^2 \theta_w \right) + N \left(-\frac{1}{2} \right) + 3(Z + N) \frac{g'F(q^2, \Lambda^2)}{q^2 + m'^2} \frac{1}{2\sqrt{2}G_F} \right], \quad (3.4)$$

We have assumed the Z' couplings are the same for the up and down quark.

On the other hand, for the scalar model, the effective interaction is

$$\mathcal{L}_{\text{BSM}} = \bar{\nu}_L^c \nu_L \bar{f} f \frac{g' F(q^2, \Lambda^2)}{q^2 + m'^2}, \quad (3.5)$$

which does not interfere with the SM. We can write its contribution to the differential cross section as

$$\frac{d\sigma}{dE_R} = \frac{d\sigma}{dE_R}|_{SM} + \frac{1}{4\pi} \left(\frac{g' F(q^2, \Lambda^2)}{q^2 + m'^2} \right)^2 \frac{E_R m_e^2}{E_\nu^2}, \quad (3.6)$$

for electron scattering, and

$$\frac{d\sigma}{dE_R} = \frac{d\sigma}{dE_R}|_{SM} + \frac{1}{4\pi} \left(\frac{(15.1Z + 14N) g' F(q^2, \Lambda^2)}{q^2 + m'^2} \right)^2 \frac{E_R m_e^2}{E_\nu^2}, \quad (3.7)$$

for nucleus scattering [9]. Here Z (N) corresponds to the number of protons (neutrons).

4 Experimental bounds

This section describes the experiments that we use to bound the aforementioned models. We begin by discussing accelerator and reactor experiments, and then discuss solar neutrino experiments.

4.1 Accelerators and reactors

To evaluate current and future constraints from accelerator and reactor CE ν NS experiments, we use a χ^2 analysis to calculate bounds on the coupling at the 2σ confidence level. To take into account reactor and accelerator neutrino flux uncertainties, we introduce a nuisance parameter α and an uncertainty on the signal of σ_α . We define

$$\chi^2 = \sum_{\text{bins}} \left[\frac{N_{obs}^i - (1 + \alpha) N_{th}^i}{\sigma_{\text{stat}}^i} \right]^2 + \left(\frac{\alpha}{\sigma_\alpha} \right)^2, \quad (4.1)$$

where N_{obs}^i (N_{th}^i) is the observed (predicted) number of events per bin in a current measurement, $\sigma_\alpha = 0.28$ and σ_{stat}^i is the statistical uncertainty which can be extracted from Ref. [1]. For future measurements with multiple detectors we define (with indices suppressed),

$$\chi^2 = \sum_{\text{bins, detectors}} \frac{(N_{SM} - (1 + \alpha) N_{th})^2}{N_{bg} + N_{SM}} + \left(\frac{\alpha}{\sigma_\alpha} \right)^2, \quad (4.2)$$

where N_{SM} is the expected number of events in the SM for a future measurement and N_{bg} is the expected number of background events, which we assume to be known precisely. Here we estimate $\sigma_\alpha = 0.1$ for future measurement.

The current COHERENT experiment has a threshold 4.25 keV [1]. For the future projected measurements we assume a threshold of 100 eV for Ge and Si reactor experiments [14–16], and 2 keV for NaI and Ar with COHERENT [17]. For reactor neutrinos

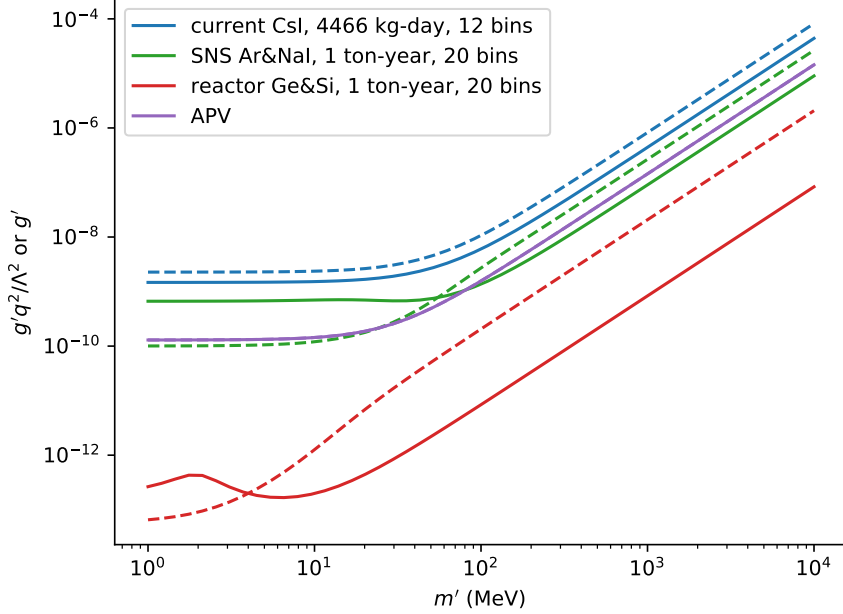


Figure 2. Current and projected 2σ bounds on a vector mediator with $F(q^2) \sim q^2$ as a function of the mediator mass. Dashed lines show the limits without a form factor. Here $q_0 = 50$ MeV for COHERENT, and $q_0 = 30$ MeV for reactor experiments.

we take a background of 1 dru (Ge and Si), and for accelerator neutrino data we take a background of 5×10^{-3} dru (CsI, NaI and Ar) [1]. Here the unit dru stands for differential rate unit, equal to event/(keV · kg · day). The COHERENT experiment has an energy dependent efficiency. We applied the efficiency function from [1] to all the detectors in the COHERENT experiment. We take the reactor neutrino flux to be that of a 1 MW reactor at ~ 1 m from the core (which yields a the total flux of 1.5×10^{12} cm²/s), and the antineutrino fission spectrum at various sites from Ref. [18]. The accelerator neutrino flux at SNS is 4.29×10^9 cm²/s [1].

In Figs. 2 and 3 we show the COHERENT and reactor constraints on $\frac{g'q^2}{\Lambda^2} = \frac{(g_L + g_R)g_\nu q_0^2}{2\Lambda^2}$ at 2σ for a vector or scalar mediator, respectively, as a function of the mediator mass. $\frac{g'q^2}{\Lambda^2}$ represents the coupling strength between quarks and neutrinos as a function of energy and reduces to g' if there is no form factor for the coupling. We choose q_0 to be a typical momentum for the experiment, e.g., $q_0 = 50$ MeV and 30 MeV are used for COHERENT and reactor experiments, respectively. To compare with the limits for the case without a form factor, we plot the corresponding limits using dashed lines. The quarks may have direct couplings to the Z' and may also couple via DM loops in a given model, in which case the solid and dashed lines must be combined to obtain constraints on the couplings. The plateau for small mediator masses arises because $m'^2 \ll q^2$ which makes the limits independent of the mediator mass. In the regime of large mediator masses, the slope of the limit curves is 2 since the effective couplings become $\frac{g'}{m'^2}$, i.e., $\log g' \propto 2 \log m'$. Also

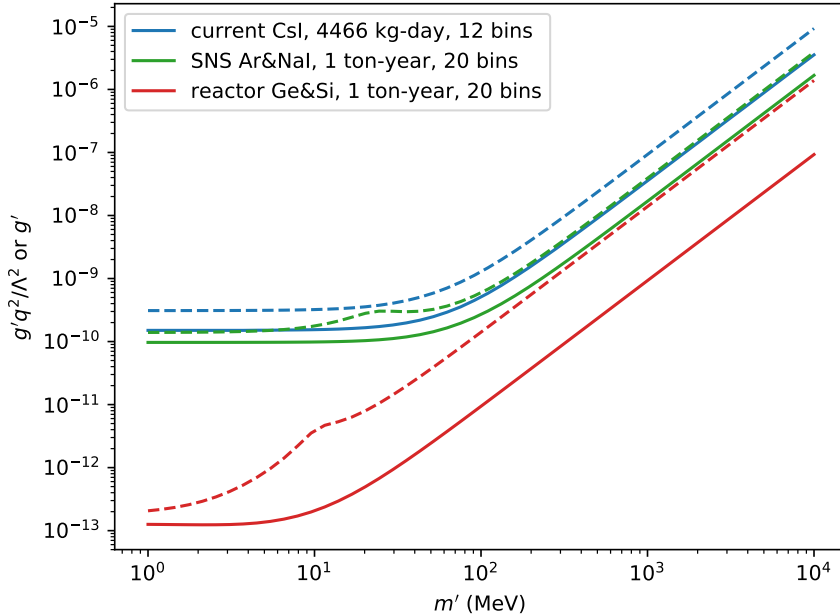


Figure 3. Current and projected 2σ bounds on a scalar mediator with $F(q^2) \sim q^2$ as a function of the mediator mass. Dashed lines show the limits without a form factor. Here $q_0 = 50$ MeV for COHERENT, and $q_0 = 30$ MeV for reactor experiments.

notice that there is a bump in the low mass region for future COHERENT and reactor experiments because a combination of the form factor and the mediator propagator yields $\frac{q^2}{q^2 + m'^2} \sim 1$, so that the mediator-induced spectral distortion is suppressed. On the other hand, for the case with no form factor, the shape distortion persists for low masses, which makes the limits stronger compared to the $F(q^2) \sim q^2$ case. Note that direct detection constraints are nonexistent for sub-GeV DM and collider bounds are nonexistent for a GeV mediator which allows a lot of the parameter space to be unconstrained for $g \leq 1$.

An effect of the form factor, $F(q^2) \sim q^2$, is that the spectral shapes differ from the SM prediction and from new physics models with $F(q^2) = 1$. To illustrate this, we show the spectrum of coherent scattering off a Ar target in Fig. 4. We choose the coupling g from current COHERENT constraints for $F(q^2) \sim q^2$ (solid line) and $F(q^2) = 1$ (dashed line). The main difference between the solid lines and dashed lines are at the higher energy end because the form factor q^2 enhances the deviation from the SM. At low energy, the spectrum is suppressed by the detection efficiency.

4.2 Solar neutrinos

Several solar neutrino experiments, for example Super-K [19], SNO [20], and Borexino [2], are sensitive to the neutrino-electron elastic scattering detection channel. Since the typical momentum transfer that solar neutrino experiments are sensitive to is ~ 0.4 MeV, it is possible to probe much smaller values of Λ as compared to reactor and accelerator CE ν NS

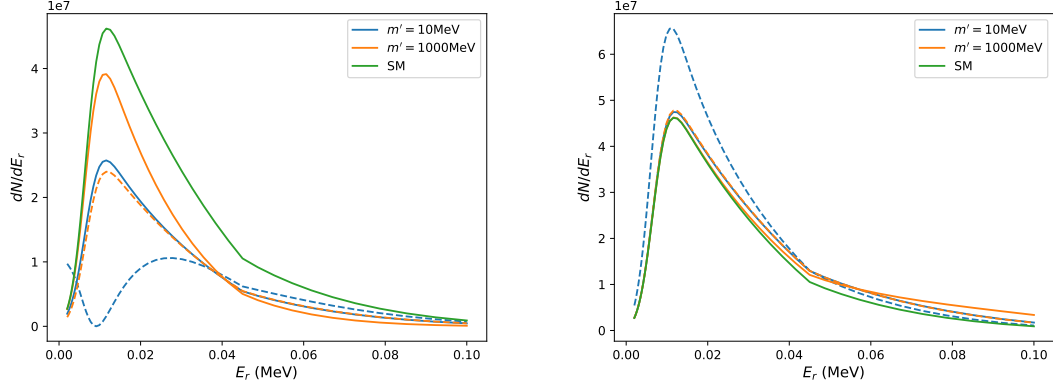


Figure 4. Spectrum of neutrino scattering off Ar detector with 1 ton–year exposure, with $\Lambda = 100$ MeV. The left panel is for the vector mediator and the right panel is for the scalar mediator. Here the couplings for non-standard interactions are taken from the bound of current COHERENT CsI limit. The dashed lines show the spectrum without a form factor.

experiments. Here we consider all the most prominent low energy components of the solar neutrino flux that Borexino is sensitive to, i.e., pp , pep , and ${}^7\text{Be}$. We choose the high metallicity solar model as defined in Ref. [21] for our baseline Standard Solar Model (SSM), and comment on the impact of the model uncertainties below.

For solar neutrino experiments, the systematic uncertainties dominate. So we define χ^2 for each component of the solar flux to be

$$\chi^2 = \frac{(N_{th} - N_{obs})^2}{N_{obs}\sigma}, \quad (4.3)$$

where σ is the percent uncertainty in the measurement (including experimental and theoretical uncertainties in quadrature) with $\sigma_{pp} = 0.11$, $\sigma_{{}^7\text{Be}} = 0.03$, and $\sigma_{pep} = 0.21$ [2]. To obtain a combined limit we define $\chi^2 = \chi_{pp}^2 + \chi_{{}^7\text{Be}}^2 + \chi_{pep}^2$.

In Figs. 5 and 6, we show the constraints on the $ee\nu\nu$ coupling from Borexino [2]. We find that the pp and ${}^7\text{Be}$ components provide the strongest constraints on $F(q^2) \sim q^2$ because of their higher event rates and smaller flux uncertainties. This is despite the fact that the pep component has larger spectral distortions (for the form-factor case relative to the $F(q^2) = 1$ case) due to its higher energy. The limit plots are valid as long as $\Lambda^2 \gg q^2$.

As for the nucleus scattering case, the recoil spectra in Fig. 7 show that the $F(q^2) \sim q^2$ case is different from the $F(q^2) = 1$ case. We see that the major differences in the spectra are at high energies. The differences for the scalar case are more significant than for the vector case because in the vector scenario the q^2 enhancement is suppressed by the interference between SM and new physics contributions.

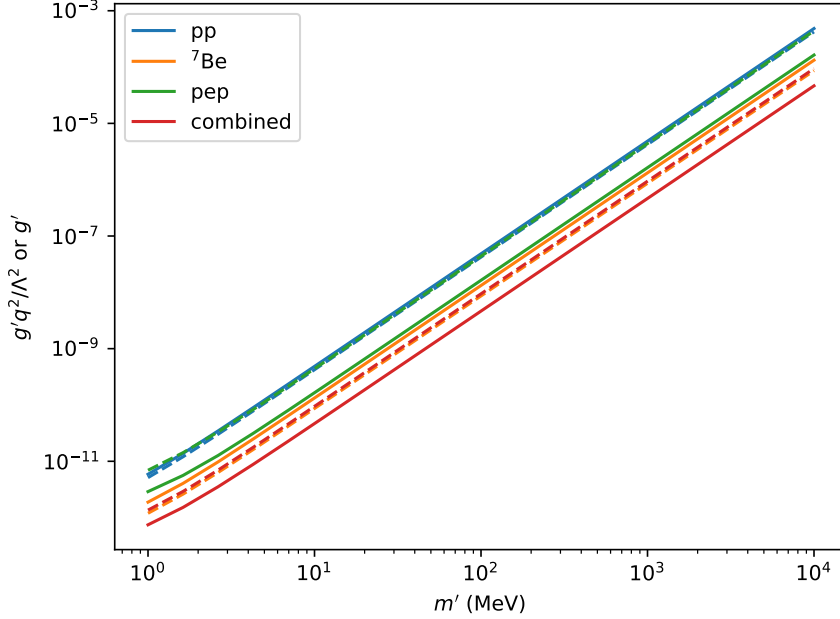


Figure 5. Constraints at 2σ from the Borexino experiment on a vector mediator with $F(q^2) \sim q^2$ as a function of the mediator mass, compared to the case of a mediator without a form factor (dashed line). We set $q = 0.5$ MeV and $\Lambda = 10$ MeV for the form factor case to compare it to the no-form-factor case.

5 B anomalies

In the SM the three families of quarks and leptons are identical except for their masses. Tests of the universality of leptonic interactions are crucial probes of new physics. Recently, hints of lepton universality violating (LUV) measurements in B decays have attracted a lot of attention. These anomalies are found in the charged current $b \rightarrow c\tau^-\bar{\nu}_\tau$ and neutral current $b \rightarrow s\ell^+\ell^-$ transitions. Here we focus on the neutral current anomalies though the anomalies might be related [22–24]. The LHCb Collaboration has measured the ratio $R_{K^*} \equiv \mathcal{B}(B^0 \rightarrow K^{*0}\mu^+\mu^-)/\mathcal{B}(B^0 \rightarrow K^{*0}e^+e^-)$ in two ranges of the dilepton invariant mass-squared q^2 [25]:

$$R_{K^*}^{\text{expt}} = \begin{cases} 0.660_{-0.07}^{+0.11} (\text{stat}) \pm 0.03 (\text{syst}), & 0.045 \leq q^2 \leq 1.1 \text{ GeV}^2, \quad (\text{low } q^2) \\ 0.69_{-0.07}^{+0.11} (\text{stat}) \pm 0.05 (\text{syst}), & 1.1 \leq q^2 \leq 6.0 \text{ GeV}^2, \quad (\text{central } q^2). \end{cases} \quad (5.1)$$

These differ from the SM by $2.2\text{--}2.4\sigma$ (low q^2) and $2.4\text{--}2.5\sigma$ (central q^2), which supports the hint of lepton nonuniversality observed earlier in a similar ratio with K mesons. The observable in this case is $R_K \equiv \mathcal{B}(B^+ \rightarrow K^+\mu^+\mu^-)/\mathcal{B}(B^+ \rightarrow K^+e^+e^-)$ [26, 27], which was measured by LHCb [28]:

$$R_K^{\text{expt}} = 0.745_{-0.074}^{+0.090} (\text{stat}) \pm 0.036 (\text{syst}), \quad 1 \leq q^2 \leq 6.0 \text{ GeV}^2, \quad (5.2)$$

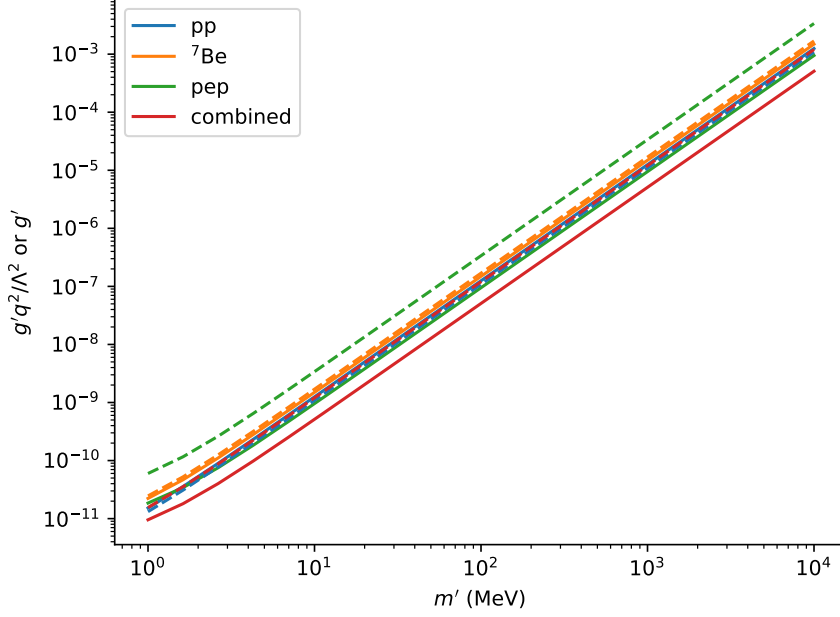


Figure 6. Constraints at 2σ from the Borexino experiment on a scalar mediator with $F(q^2) \sim q^2$ as a function of the mediator mass, compared to the case of a mediator without a form factor (dashed line). We set $q = 0.5$ MeV and $\Lambda = 10$ MeV for the form factor case to compare it to the no-form-factor case.

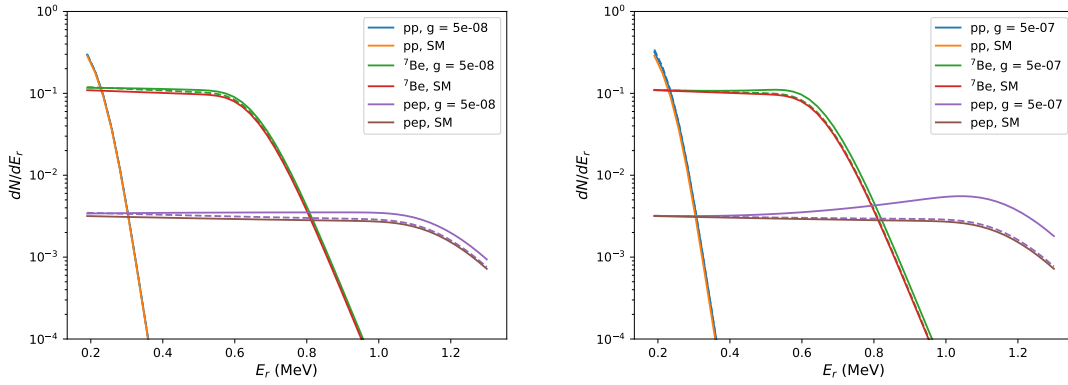


Figure 7. Spectra of solar neutrino scattering off electrons, with $m' = 10$ MeV and $\Lambda = 10$ MeV, and scaled to match the Borexino measurement. The left panel is for the vector mediator and the right panel is for the scalar mediator. Dashed lines are the spectra without a form factor. To make a fair comparison, for the latter case we scale g by a factor of q^2/Λ^2 .

and found to differ from the SM prediction, $R_K^{\text{SM}} = 1 \pm 0.01$ [29] by 2.6σ . Other anomalies also appear in the branching ratios and angular observables of certain $b \rightarrow s\mu^+\mu^-$ decays.

While many new physics models with new heavy states have been discussed to address these anomalies, it was pointed out that new physics with light mediators could also explain these anomalies [30]. In particular, with heavy new physics it is difficult to understand the R_{K^*} measurement in the low q^2 bin, $0.045 \leq q^2 \leq 1.1 \text{ GeV}^2$, along with the measurement of R_{K^*} in the central q^2 bin and the measurement of R_K .

For light new physics in the MeV range a resolution of the R_K and R_{K^*} measurements in the central q^2 bin along with other angular observables in $b \rightarrow s\mu^+\mu^-$ decays is possible with the light states coupling only to muons [3, 30, 31]. In addition, in this framework the discrepancy in the anomalous magnetic moment of the muon can also be explained and there are interesting implications for nonstandard neutrino interactions. However, the measurement of R_{K^*} in the low q^2 bin cannot be satisfactorily explained. For the model to work a nontrivial form factor for the flavor changing bsX vertex is required, where X is a light state. This can happen if the bsX coupling is induced at loop level due to some additional light new physics [3] just as we have considered in the case of neutrino scattering. To explain the R_K and R_{K^*} in all bins with a light mediator is difficult and requires X to couple to electrons rather than muons [3]. In this case the anomalies in the angular observables in $b \rightarrow s\mu^+\mu^-$ decays remain unexplained. This might suggest that there is different new physics responsible for measurements in different q^2 bins. One can also aim to understand only the low q^2 bin R_{K^*} measurement and such an approach is followed in Ref. [32].

It is possible to connect B decays to coherent neutrino scattering by generalizing Eq. (2.1) to include all generations of quarks. We write the modified Lagrangian as

$$\begin{aligned}\mathcal{L} &= \frac{g}{\Lambda^2} \bar{q}' i \gamma^\mu P_{L,R} Y_{U,D}^{i,j} q'_j \bar{\chi} \gamma_\mu (1 \pm \gamma_5) \chi + i \bar{\chi} \gamma^\nu [\partial_\nu - i g_\chi Z'^\nu] \chi - m_\chi \bar{\chi} \chi + \frac{1}{2} m_{Z'}^2 Z'_\mu Z'^\mu \\ &= H_{eff} + J_{\mu,\chi} Z'^\mu + i \bar{\chi} \gamma^\nu \partial_\nu \chi - m_\chi \bar{\chi} \chi + \frac{1}{2} m_{Z'}^2 Z'_\mu Z'^\mu,\end{aligned}\tag{5.3}$$

where i, j are the family indices and $Y_{U,D}$ are the flavor couplings for the up and down quarks. To simplify the discussion we assume that only the left-handed quarks are involved in the interactions with the χ fields. However, in order to satisfy the R_K and R_{K^*} anomalies we need flavor violation in the $b-s$ sector arising from the following Yukawa matrices:

$$\begin{aligned}Y_D &= \begin{pmatrix} g_1 & 0 & 0 \\ 0 & a_1 & b_1 \\ 0 & b_1 & c_1 \end{pmatrix}, \\ Y_U &= V_{CKM} Y_D V_{CKM}^\dagger,\end{aligned}\tag{5.4}$$

The origin of the texture in the $Y_{U,D}$ can be understood by introducing a new gauge symmetry motivated by a $U(1)_{\mu-\tau}$ model [33–36], and including the quark sector. We assume that the Lagrangian has a similar symmetry in the quark sector with the following new Yukawa terms: $\lambda_1^d \bar{Q}_L^{(2)} \tilde{H}_3 D_R^{(3)} + \lambda_2 \bar{Q}_L^{(3)} \tilde{H}_4 D_R^{(2)}$, where $\tilde{H}_{3,4}$ have new gauge charges $2a, -2a$ respectively, in addition to the SM weak charge assignments $(2, 1/2)$ under $SU(2)_L$ and $U(1)_Y$. Similar terms for the up sector are present as well. Such a model has been

constructed in Ref. [37]. Here we assume that the quarks transform as $(0, a, -a)$ but we could have assumed $(a, a, -2a)$ as well with different charge assignments for the new Higgs.

In the weak interaction basis, the couplings to Z' associated with the new symmetry is diagonal,

$$Y'_{U,D} = \begin{pmatrix} g_1 & 0 & 0 \\ 0 & g_2 & 0 \\ 0 & 0 & g_3 \end{pmatrix}. \quad (5.5)$$

In transforming from the gauge basis to the mass basis (with the contributions arising from the off-diagonal terms in the Lagrangian), we write

$$u'_L = U_L u_L, \quad d'_L = D_L d_L, \quad (5.6)$$

where U_L and D_L are 3×3 unitary matrices for the up and down quarks respectively, and the spinors $u^{(\prime)}$ and $d^{(\prime)}$ include all three generations of fermions. The CKM matrix is given by $V_{CKM} = U_L^\dagger D_L$ and after transforming to the mass basis we can rewrite Eq. (5.3) with the $Y'_{U,D}$ matrices replaced by $Y_D = D_L^\dagger Y'_D D_L$ and $Y_U = U_L^\dagger Y'_U U_L$. Now if all the mixing is in the up sector with $D_L = I$ then there is no FCNC in the down sector. To generate the $b \rightarrow s$ transition we use the assumption of Ref. [38] that D_L involves only the second and third generations:

$$D_L = \begin{pmatrix} 1 & 0 & 0 \\ 0 & \cos \theta_D & \sin \theta_D \\ 0 & -\sin \theta_D & \cos \theta_D \end{pmatrix}. \quad (5.7)$$

The $Y_{U,D}$ matrices then have the explicit form,

$$Y_D = \begin{pmatrix} g_1 & 0 & 0 \\ 0 & c_D^2 g_2 + s_D^2 g_3 & c_D s_D (g_2 - g_3) \\ 0 & c_D s_D (g_2 - g_3) & c_D^2 g_3 + s_D^2 g_2 \end{pmatrix},$$

$$Y_U = V_{CKM} Y_D V_{CKM}^\dagger, \quad (5.8)$$

where $c_D \equiv \cos \theta_D$ and $s_D \equiv \sin \theta_D$. We see that in the down sector flavor changing $b \rightarrow s$ transitions occur with coupling $g_{bs} = c_D s_D (g_2 - g_3)$. The form factor for coherent scattering is $F(q^2) = g_L \frac{q^2}{\Lambda^2}$ while for the B decays it is $F(q^2) = g_{Lbs} \frac{q^2}{\Lambda^2}$ with $g_L \propto g_1$, $g_{Lbs} \propto g_{bs}$ and $\frac{g_1}{g_{bs}} = \frac{g_L}{g_{Lbs}}$. If all the g_i are of the same order of magnitude then $g_{Lbs} < g_L$.

The breakdown of lepton flavor universality required for the $R_{K^{(*)}}$ anomaly can arise in $U(1)_{\mu-\tau}$ symmetry models. We now compare the flavor violating terms with the flavor conserving terms in the quark sector.

Combining the B decay anomalies with the results from coherent scattering allows us to check for the consistency of this framework. We focus on the Z' models. Figure 2 gives the bound on the diagonal term using the COHERENT experiment,

$$\Lambda^2 > q_0^2 \frac{g_L g_\mu}{X_l}, \quad (5.9)$$

where g_μ is the Z' coupling to muon neutrinos, and we can read off X_l from the figure.

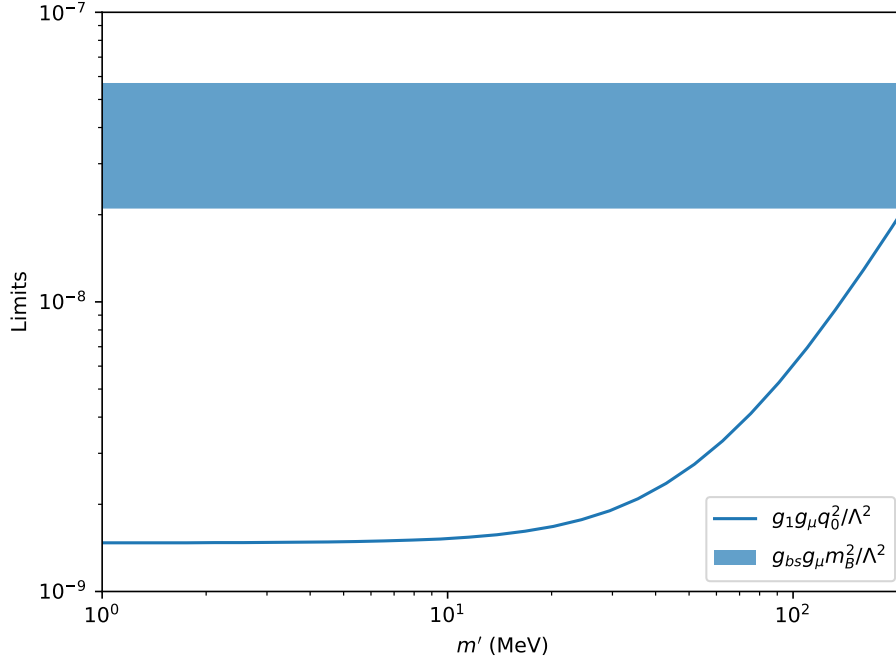


Figure 8. Scale (Λ) independent comparison between current 2σ COHERENT and 1σ B decay constraints on diagonal or off-diagonal couplings for a mediator lighter than $2m_\mu$.

We now turn our attention to the $R_{K^{(*)}}$ anomaly which involves a flavor violating $b-s$ interaction with charged muons. Using the recent results on $R_{K^{(*)}}$, we obtain a constraint on the flavor violating term. We assume the left handed leptons have identical couplings and so g_μ can be fixed from the muon anomalous magnetic moment measurement and neutrino trident production. Using $g_\mu \sim 10^{-3}$ [3, 31] and $X_l \sim 10^{-9}$ from Fig. 2 we obtain

$$\Lambda > 10^3 q_0 g_L, \quad (5.10)$$

which gives $\Lambda > 50 g_L$ GeV for $q_0 = 50$ MeV. In B decays the relevant q_0 is taken to be m_B and so with the additional assumption of $SU(2)_L$ symmetry for the left handed leptonic couplings we obtain [3],

$$g_{Lbs} \frac{m_B^2}{\Lambda^2} g_\mu \sim X_h. \quad (5.11)$$

Combining this with Eq. (5.9), we get

$$\frac{g_{Lbs}}{g_L} = \frac{g_{bs}}{g_1} > \frac{X_h}{X_l} \frac{q_0^2}{m_B^2}. \quad (5.12)$$

Using $X_h \sim 10^{-8}$ [3] and $X_l \sim 10^{-9}$ from Fig. 8, we find $g_{bs}/g_1 \sim 10^{-3}$ for m' between 1 – 10 MeV, and $g_{bs}/g_1 \sim 10^{-4}$ for $m' = 100$ MeV. However, if the bounds from coherent scattering get stronger, then $\frac{g_{Lbs}}{g_L}$ will increase and lead to tension in the framework. A similar analysis can also be done with scalar mediators where tighter constraints are obtained.

The B anomalies also indicate lepton universality violating new physics which will be interesting to check in neutrino scattering. For instance if the $R_{K^{(*)}}$ anomalies are explained with mediators coupling differently to muons and electrons then ν_μ and ν_e scattering may show different new physics effects.

6 Conclusions

We have explored the limits of the effective couplings arising from a high energy scale (Λ) hidden sector associated with dark matter. We considered two general models which give rise to a coupling form factor that is proportional to the momentum q^2 . The Z' model corresponds to vector couplings between neutrinos and quarks, and the S model corresponds to scalar couplings. At low energies, we have shown that it is possible to probe Λ via CE ν NS experiments via the form factor which is induced by a DM (χ) loop. We considered scenarios in which Λ is ≥ 50 MeV, and in which the energy scale is ≤ 1 MeV. CE ν NS experiments can probe the former case since Λ is higher than the momentum transfer but these experiments are unable to probe the latter case. To probe the scenario with small Λ , we used solar electron scattering experiments for which the momentum transfer is low.

In the Z' model, COHERENT constrains the coupling to be $\sim 10^{-8}$ at 2σ for small mediator masses. For large mediator masses, the bound scales according to $\log g' \propto 2 \log m'$, as shown in Fig. 4.1. Atomic parity violation does better than most of the CE ν NS experiments except those using reactor neutrinos. For small Λ the Borexino experiment puts 2σ constraints on the couplings $\mathcal{O}(10^{-7})$ for a 100 MeV mass mediator. Since the momentum transfer is much smaller, the constraints scale like $\log g' \propto 2 \log m'$ as shown in Fig. 5.

In the S model, COHERENT constrains the coupling to be $\sim 10^{-9}$ for small mediator masses. For large mediator masses, the bound scales according to $\log g' \propto 2 \log m'$, as shown in Fig. 4.2. Atomic parity violation experiments do not constrain models with scalar mediators. For small Λ , the Borexino experiment puts 2σ constraints on the couplings $\mathcal{O}(10^{-7})$ for a 100 MeV mass mediator. Since the momentum transfer is much smaller, the constraints scale like $\log g' \propto 2 \log m'$ as shown in Fig. 6.

Finally, we have extended our framework to quarks of all generations and have addressed the R_K and R_{K^*} anomalies in rare B decays. We have shown that a resolution of the anomalies consistent with the present coherent scattering data is possible but future constraints from coherent scattering will provide stringent tests of the B anomalies explanation.

Acknowledgements

A.D. acknowledges the hospitality of University of California, Irvine where this work was completed. D.M. thanks the Mitchell Institute at Texas A&M University for its support and hospitality while this work was in progress. A.D. acknowledges support from NSF under Grant No. PHY-1414345. B.D. and L.S. acknowledge support from DOE Grant de-sc0010813. S.L. acknowledges support from TAMU - College of Science - STRP. D.M. acknowledges support from DOE Grant No. de-sc0010504.

References

- [1] COHERENT collaboration, D. Akimov et al., *Observation of Coherent Elastic Neutrino-Nucleus Scattering*, *Science* **357** (2017) 1123 [[1708.01294](#)].
- [2] BOREXINO collaboration, M. Agostini et al., *First Simultaneous Precision Spectroscopy of pp, ^7Be , and pep Solar Neutrinos with Borexino Phase-II*, [1707.09279](#).
- [3] A. Datta, J. Kumar, J. Liao and D. Marfatia, *New light mediators for the R_K and R_{K^*} puzzles*, *Phys. Rev.* **D97** (2018) 115038 [[1705.08423](#)].
- [4] J. Goodman, M. Ibe, A. Rajaraman, W. Shepherd, T. M. P. Tait and H.-B. Yu, *Constraints on Dark Matter from Colliders*, *Phys. Rev.* **D82** (2010) 116010 [[1008.1783](#)].
- [5] Y. Bai, P. J. Fox and R. Harnik, *The Tevatron at the Frontier of Dark Matter Direct Detection*, *JHEP* **12** (2010) 048 [[1005.3797](#)].
- [6] J. Fan, M. Reece and L.-T. Wang, *Non-relativistic effective theory of dark matter direct detection*, *JCAP* **1011** (2010) 042 [[1008.1591](#)].
- [7] G. Elor, H. Liu, T. R. Slatyer and Y. Soreq, *Complementarity for Dark Sector Bound States*, [1801.07723](#).
- [8] A. Datta, M. Duraisamy and D. Ghosh, *Explaining the $B \rightarrow K^* \mu^+ \mu^-$ data with scalar interactions*, *Phys. Rev.* **D89** (2014) 071501 [[1310.1937](#)].
- [9] D. G. Cerdeno, M. Fairbairn, T. Jubb, P. A. N. Machado, A. C. Vincent and C. Bahm, *Physics from solar neutrinos in dark matter direct detection experiments*, *JHEP* **05** (2016) 118 [[1604.01025](#)].
- [10] M. Cirelli, E. Del Nobile and P. Panci, *Tools for model-independent bounds in direct dark matter searches*, *JCAP* **1310** (2013) 019 [[1307.5955](#)].
- [11] PARTICLE DATA GROUP collaboration, M. Tanabashi et al., *Review of Particle Physics*, *Phys. Rev.* **D98** (2018) 030001.
- [12] Y. Nambu and G. Jona-Lasinio, *Dynamical Model of Elementary Particles Based on an Analogy with Superconductivity. 1.*, *Phys. Rev.* **122** (1961) 345.
- [13] D. Aristizabal Sierra, B. Dutta and L. Strigari, *In preparation*, (2019) .
- [14] CONNIE collaboration, A. Aguilar-Arevalo et al., *The CONNIE experiment*, *J. Phys. Conf. Ser.* **761** (2016) 012057 [[1608.01565](#)].
- [15] TEXONO collaboration, H. Bin Li, *Neutrino and dark matter physics with sub-KeV Germanium detectors*, *J. Phys. Conf. Ser.* **718** (2016) 062036.
- [16] MINER collaboration, G. Agnolet et al., *Background Studies for the MINER Coherent Neutrino Scattering Reactor Experiment*, *Nucl. Instrum. Meth.* **A853** (2017) 53 [[1609.02066](#)].
- [17] COHERENT collaboration, D. Akimov et al., *COHERENT 2018 at the Spallation Neutron Source*, [1803.09183](#).
- [18] DAYA BAY collaboration, F. P. An et al., *Improved Measurement of the Reactor Antineutrino Flux and Spectrum at Daya Bay*, *Chin. Phys.* **C41** (2017) 013002 [[1607.05378](#)].
- [19] SUPER-KAMIOKANDE collaboration, K. Abe et al., *Solar neutrino results in Super-Kamiokande-III*, *Phys. Rev.* **D83** (2011) 052010 [[1010.0118](#)].

- [20] SNO collaboration, B. Aharmim et al., *Combined Analysis of all Three Phases of Solar Neutrino Data from the Sudbury Neutrino Observatory*, *Phys. Rev.* **C88** (2013) 025501 [[1109.0763](#)].
- [21] W. C. Haxton, R. G. Hamish Robertson and A. M. Serenelli, *Solar Neutrinos: Status and Prospects*, *Ann. Rev. Astron. Astrophys.* **51** (2013) 21 [[1208.5723](#)].
- [22] B. Bhattacharya, A. Datta, D. London and S. Shivashankara, *Simultaneous Explanation of the R_K and $R(D^{(*)})$ Puzzles*, *Phys. Lett.* **B742** (2015) 370 [[1412.7164](#)].
- [23] A. Greljo, G. Isidori and D. Marzocca, *On the breaking of Lepton Flavor Universality in B decays*, *JHEP* **07** (2015) 142 [[1506.01705](#)].
- [24] A. Crivellin, D. Muller and T. Ota, *Simultaneous explanation of $R(D^{(*)})$ and $b \rightarrow s\mu^+\mu^-$: the last scalar leptoquarks standing*, *JHEP* **09** (2017) 040 [[1703.09226](#)].
- [25] LHCb collaboration, R. Aaij et al., *Test of lepton universality with $B^0 \rightarrow K^{*0}\ell^+\ell^-$ decays*, *JHEP* **08** (2017) 055 [[1705.05802](#)].
- [26] G. Hiller and F. Kruger, *More model-independent analysis of $b \rightarrow s$ processes*, *Phys. Rev.* **D69** (2004) 074020 [[hep-ph/0310219](#)].
- [27] G. Hiller and M. Schmaltz, *R_K and future $b \rightarrow s\ell\ell$ physics beyond the standard model opportunities*, *Phys. Rev.* **D90** (2014) 054014 [[1408.1627](#)].
- [28] LHCb collaboration, R. Aaij et al., *Test of lepton universality using $B^+ \rightarrow K^+\ell^+\ell^-$ decays*, *Phys. Rev. Lett.* **113** (2014) 151601 [[1406.6482](#)].
- [29] M. Bordone, G. Isidori and A. Pattori, *On the Standard Model predictions for R_K and R_{K^*}* , *Eur. Phys. J.* **C76** (2016) 440 [[1605.07633](#)].
- [30] A. Datta, J. Liao and D. Marfatia, *A light Z' for the R_K puzzle and nonstandard neutrino interactions*, *Phys. Lett.* **B768** (2017) 265 [[1702.01099](#)].
- [31] A. K. Alok, B. Bhattacharya, A. Datta, D. Kumar, J. Kumar and D. London, *New Physics in $b \rightarrow s\mu^+\mu^-$ after the Measurement of R_{K^*}* , *Phys. Rev.* **D96** (2017) 095009 [[1704.07397](#)].
- [32] W. Altmannshofer, M. J. Baker, S. Gori, R. Harnik, M. Pospelov, E. Stamou et al., *Light resonances and the low- q^2 bin of R_{K^*}* , *JHEP* **03** (2018) 188 [[1711.07494](#)].
- [33] C. S. Lam, *A 2-3 symmetry in neutrino oscillations*, *Phys. Lett.* **B507** (2001) 214 [[hep-ph/0104116](#)].
- [34] T. Kitabayashi and M. Yasue, *$S(2L)$ permutation symmetry for left-handed mu and tau families and neutrino oscillations in an $SU(3)$ -L \times $SU(1)$ -N gauge model*, *Phys. Rev.* **D67** (2003) 015006 [[hep-ph/0209294](#)].
- [35] W. Grimus and L. Lavoura, *A Discrete symmetry group for maximal atmospheric neutrino mixing*, *Phys. Lett.* **B572** (2003) 189 [[hep-ph/0305046](#)].
- [36] Y. Koide, *Universal texture of quark and lepton mass matrices with an extended flavor 2 \leftrightarrow 3 symmetry*, *Phys. Rev.* **D69** (2004) 093001 [[hep-ph/0312207](#)].
- [37] A. Datta and P. J. O'Donnell, *The 2-3 symmetry: Flavor changing b , tau decays and neutrino mixing*, *Phys. Rev.* **D72** (2005) 113002 [[hep-ph/0508314](#)].
- [38] B. Bhattacharya, A. Datta, J.-P. Gu  vin, D. London and R. Watanabe, *Simultaneous Explanation of the R_K and $R_{D^{(*)}}$ Puzzles: a Model Analysis*, *JHEP* **01** (2017) 015 [[1609.09078](#)].